

Occam’s model: Selecting simpler representations for better transferability estimation

Prabhat Singh ^{* 1} Sibylle Hess ^{* 1} Joaquin Vanschoren ^{* 1}

Abstract

Fine-tuning models that have been pre-trained on large datasets has become a cornerstone of modern machine learning workflows. With the widespread availability of online model repositories, such as Hugging Face, it is now easier than ever to fine-tune pre-trained models for specific tasks. This raises a critical question: which pre-trained model is most suitable for a given task? This problem is called transferability estimation. In this work, we introduce two novel and effective metrics for estimating the transferability of pre-trained models. Our approach is grounded in viewing transferability as a measure of how easily a pre-trained model’s representations can be trained to separate target classes, providing a unique perspective on transferability estimation. We rigorously evaluate the proposed metrics against state-of-the-art alternatives across diverse problem settings, demonstrating their robustness and practical utility. Additionally, we present theoretical insights that explain our metrics’ efficacy and adaptability to various scenarios. We experimentally show that our metrics increase Kendall’s Tau by up to 32% compared to the state-of-the-art baselines.

1. Introduction

Using models pre-trained on large datasets like ImageNet (Deng et al., 2009) has become a standard practice in real-world deep-learning scenarios. For example, the top five models on HuggingFace have been downloaded more than 200M times. HuggingFace hosts more than 15K models for image classification. The performance and efficiency gain from using models pre-trained on large datasets like ImageNet 21k (Deng et al., 2009) and LIAON (Schuhmann et al., 2022) is enormous. However, these performance gains can vary considerably depending on model architecture, weights, and the dataset it was pre-trained on (source dataset). This leads to the pre-trained model selection problem. Although the model selection task has strong roots in AutoML, applying classic model selection paradigms is

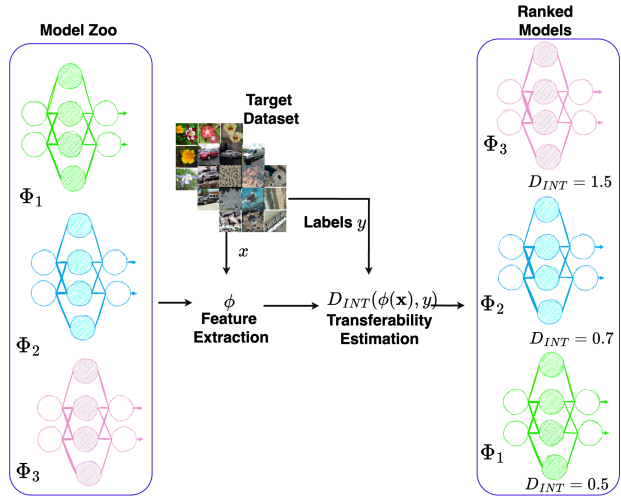


Figure 1. Given a set of pre-trained models and a target dataset, extract the embeddings and estimate a complexity score D_{INT} to rank pre-trained models based on their suitability for the target task.

computationally too expensive in this scenario. Fine-tuning each model on the target data for a search strategy like Bayesian optimization is not feasible since the fine-tuning step is too expensive. This raises the question: *“How can we find a high-performing pre-trained model for a given target task without fine-tuning our models and without access to the source dataset.”*

This question is answered by transferability estimation methods. The idea behind transferability estimation is to assign a score to each pre-trained model of a given set for a target task, such that one can select the top-performing model for the given task. In the last decade, there have been multiple works, addressing this problem from various perspectives. For example, TransRate (Huang et al., 2022) treats the problem from an information theory point of view, and ETran connects the problem of transferability estimation to energy-based models. There have been numerous methods that treat this problem from multiple perspectives like linearization, Bayesian modeling, matrix analysis, etc. However, we found that these approaches fall short in many practical scenarios.

In this work, we introduce a new transferability estimation

metrics by analyzing how easily a pre-trained model’s representations separate target classes. A well-trained model should produce embeddings where class distinctions are approximately clear, reducing what we call ‘representational complexity’. Recent work by Kam Ho (2022) uses data complexity measures by Ho & Basu (2002) to evaluate this notion of representational complexity and shows how data complexity evolves through the network and how it changes during training. We show that we can evaluate representational complexity by assessing interclass separation and concept variance.

In this work we were inspired by the work in cluster separation and concept variance, leading us to derive two new transferability estimation metrics. We treat the embeddings of the target task from the pre-trained model and true labels to compute our transferability metrics. We examine the embeddings generated for an unseen task by a pre-trained network and assess how challenging the task is for the network to fine-tune. Our first solution treats this problem as a clustering quality problem and the second one treats it as a Concept Variance problem. We compare performance of our metrics with the current state of the art from various families of metrics. Our solutions outperform current state-of-the-art metrics. We also show the effectiveness of our methods in a new challenging search space with modern neural networks and complex datasets in two different settings. In conclusion, this work In conclusion in this work:

- We introduce two different metrics for transferability estimation, INT and Concept Variance.
- We propose a new and challenging experimental benchmark for robust evaluation of transferability estimation metrics in multi-domain(7 domains) image classification settings with modern neural networks. We show that our method outperforms current state-of-the-art metrics with a significant increase in Kendall’s tau τ_ω (32%).
- We present theory and insight behind the effectiveness of our methods.

2. Related work

The idea behind transferability estimation is simple: to estimate which model from a zoo would perform best after fine-tuning the model. Transferability estimation as a field is fairly new, the H-Score (Bao et al., 2019) and NCE (Tran et al., 2019) can be considered as early works on this topic, introducing the evaluation of transferability, and the assignment of models corresponding to an estimate of their transferability, for a given target task.

There are two widely accepted problem scenarios for transferability estimation: source-dependent transferability es-

timation (where one has access to the source and target dataset) and source-independent transferability estimation (where one does not have access to the source dataset).

2.1. Source Dependent Transferability Estimation (SDTE)

The SDTE scenario assumes access to the source data sets where the models have been pre-trained. Apart from the fact that this assumption is often not met, a drawback of common SDTE metrics, they use distribution matching methods like optimal transport (Tan et al., 2021), which are typically very expensive to compute. In addition, SDTE metrics are usually not reliable when the discrepancy between the source and target dataset is very high, for example, when comparing entire the ImageNet21K (Deng et al., 2009) to Cars (Krause et al., 2013) or Plants (G. & J., 2019) dataset.

2.2. Source Independent Transferability Estimation(SITE)

The Source Independent Transferability Estimation (SITE) assumes access to the source model but not the source training data. This is a more realistic transferability estimation as we might not always have access to the source dataset, nor have the capacity to store the typically very large source datasets like ImageNet (Deng et al., 2009) or LAION (Schuhmann et al., 2022) in our local setup. SITE methods typically rely on evaluating the feature representation of the source model on the target dataset and its relationship with target labels.

There are several transferability metrics inspired by various viewpoints. LogME (You et al., 2021) formalizes the transferability estimation as the maximum label marginalized likelihood and adopts a directed graphical model to solve it. SFDA (Shao et al., 2022) proposes a self-challenging mechanism, it first maps the features and then calculates the sum of log-likelihood as the metric. ETran (Gholami et al., 2023) and PED (Li et al., 2023) treat the problem of SITE with an energy function, ETran uses energy-based models to detect whether a target dataset is in-distribution or out of distribution for a given pre-trained model whereas PED utilizes potential energy function to modify feature representations to aid other transferability metrics like LogMe and SFDA. NCTI (Wang et al., 2023) treats it as a nearest centroid classifier problem and measures how close the geometry of the target features is to their hypothetical state in the terminal stage of the fine-tuned model. LEEP (Nguyen et al., 2020) is the average log-likelihood of the log-expected empirical predictor, which is a non-parameter classifier based on the joint distribution of the source and target distribution, NLEEP (Li et al., 2021b) is a further improvement on LEEP by substituting the output layer with a Gaussian mixture model. TransRate (Huang et al., 2022) treats SITE from an

information theory point of view by measuring the transferability as the mutual information between features of target examples extracted by a pre-trained model and their labels. We suggest the survey by Ding et al. (2024) for a complete view of transferability metrics.

Of these existing methods, the approach of NCTI is closest to ours. NCTI checks to which extent the neural collapse criteria (Papyan et al., 2020) are satisfied on the target embedding. We argue (in Section 3.2) that neural collapse is a byproduct of properties of the loss function, that incentivize in later training stages the embedded points of one class to collapse to their mean. However, if we want to assess the transferability, checking for effects taking place late in training might not be a failproof approach.

3. Occam's model: Transferability Estimation with finding simpler representation

3.1. Problem statement

We assume that we are given a target dataset $\mathcal{D} = \{(\mathbf{x}_n, y_n)\}_{n=1}^N$ of N labeled points and M pre-trained models $\{\Phi_m = (\phi_m, \psi_m)\}_{m=1}^M$. Each model Φ_m consists of a feature extractor that returns a d -dimensional embedding $\phi_m(x) \in \mathbb{R}^d$ and the final layer or head ψ_m that outputs the label prediction for the given input x . The task of estimating transferability is to generate a score for each pre-trained model so that the best model can be identified via a ranking list. For each pre-trained model Φ_m a transferability metric outputs a scalar score T_m that should be coherent in its ranking with the performance of the fine-tuned classifier $\hat{\Phi}_m$. That is, the goal is to obtain scores T_m such that

$$T_m \geq T_n \Leftrightarrow \frac{1}{N} \sum_{n=1}^N p(y_n | \mathbf{x}_n; \hat{\Phi}_m) \geq \frac{1}{N} \sum_{n=1}^N p(y_n | \mathbf{x}_n; \hat{\Phi}_n),$$

where $p(y_n | \mathbf{x}_n; \hat{\Phi}_m)$ indicates the probability that the fine-tuned model $\hat{\Phi}_m$ predicts label y_n for input \mathbf{x}_n . A larger T_m indicates better performance model on target data \mathcal{D} .

In this work, we aim to assess transferability by finding the degree of simplicity of our representations. We hypothesize that a classifier can be more easily fine-tuned subject to a target dataset if the embedding $\{\phi(\mathbf{x}_n) \mid 1 \leq n \leq N\}$ already has a simple structure in relationship to the labels. As a simple structure, we consider for example an embedding where the points exhibit clustering properties, where the clusters coincide with the classes, or a simple distribution of points in one class. Correspondingly, we define our metrics, one that is inspired by clustering properties (Bezdek & Pal, 1998) and one that is motivated by concept characterization and variation (Rendell & Cho, 1990; Pérez & Rendell, 1996).

3.2. Clustering Approach: Measuring cluster separability as a means of transferability

Deep neural network classifiers are trained with the cross-entropy loss. Given a classifier $f_\theta : \mathbb{R}^d \rightarrow [0, 1]^C$, indicating the confidence $f_\theta(\mathbf{x})_c$ for class $1 \leq c \leq C$ and input \mathbf{x} , the cross-entropy loss is defined as

$$CE(y, f_\theta) = -\frac{1}{N} \sum_{n=1}^N \log f_\theta(\mathbf{x}_n)_{y_n}.$$

The classifier f_θ can be seen as a softmax regression (multinomial logistic regression) classifier $h_{W,b}(\mathbf{z}) = \text{softmax}(W\mathbf{z} + b)$ applied to an embedding $\phi(\mathbf{x})$. This way, we write $f_\theta(\mathbf{x}) = h(\phi(\mathbf{x}))$.

The cross entropy loss is low if there exist vectors $W_{\cdot,y}$ and biases b_y for each class y , such that the linear function value $W_{\cdot,c}^\top \mathbf{z} + b_c$ achieves its maximum value for points from class y at $c = y$. If we want to estimate how well a multinomial logistic regression model would fit the embeddings $\phi(\mathbf{x})$, then we could try to train a multinomial logistic regression on the target embedding. However, this procedure does not take into account that the embedding is flexible. Small changes in the embedding, performed during finetuning, have possibly big impacts on the classifier accuracy. Hence, we rather want to estimate how close the embedding is to a representation that is well-classifiable.

To gain insights into the classifiability of an embedding, we consider the formulation of the multinomial logistic regression objective as a Linear Discriminant Analysis (LDA) model.

Theorem 3.1. *For any multinomial regression model $h_{W,b}(\mathbf{z}) = \text{softmax}(W\mathbf{z} + b)$ exist class centers μ_1, \dots, μ_C such that*

$$h_{W,b}(\mathbf{x})_y = \frac{\exp(-\frac{1}{2}\|\mathbf{x} - \mu_y\|^2)}{\sum_{c=1}^C \exp(-\frac{1}{2}\|\mathbf{x} - \mu_c\|^2)}$$

The proof can be found in Appendix A. The theorem shows that we can analyze the classifier's performance also from the viewpoint of a nearest-center classifier. This formulation is close to unsupervised objectives such as k -means and it explains the effect of neural collapse (Papyan et al., 2020). Once the class boundaries are sufficiently optimized, meaning that the class centers don't change much anymore, the objective still incentivizes the embedded points to be close to its class center. Over time, the class centers hence become centroids and the effects of neural collapse are taking place.

The cross entropy for point \mathbf{x}_n with label y_n is equal to

$$\begin{aligned} -\log f_\theta(\mathbf{x}_n)_{y_n} &= -\log \frac{\exp(-\frac{1}{2}\|\phi(\mathbf{x}_n) - \mu_{y_n}\|^2)}{\sum_{c=1}^C \exp(-\frac{1}{2}\|\mathbf{x}_n - \mu_c\|^2)} \\ &= \log \sum_{c \neq y_n} \exp(-\frac{1}{2}\|\phi(\mathbf{x}_n) - \mu_c\|^2) \\ &\approx \max_{c \neq y_n} -\frac{1}{2}\|\phi(\mathbf{x}_n) - \mu_c\|^2. \end{aligned}$$

As a result, the loss is minimized if the embedded points of class y_n are far away from the other class centers. Since we do not know the class centers, we propose to evaluate instead the proximity of points between classes, that is equivalent to maximizing the distance to other class centers when the class centers are actually centroids.

Definition 3.2. For two classes a and b , the *Normalized Interclass Distance* between those classes is given as

$$D_{ab} = \sum_{y_i=a} \sum_{y_j=b} \frac{\text{dist}(\mathbf{x}_i, \mathbf{x}_j)}{|\{k \mid y_k = a\}| |\{l \mid y_l = b\}|}. \quad (1)$$

The *Pairwise Normalized Interclass Distances* on dataset \mathcal{D} with C classes are defined as

$$\text{INT}(\mathcal{D}) = \sum_{1 \leq a \neq b \leq C} D_{ab} \quad (2)$$

If we choose $\text{dist}(\mathbf{x}_i, \mathbf{x}_j) = \|\mathbf{x}_i - \mathbf{x}_j\|^2$, then the normalized interclass distance is equal to a normalized distance of points to the class-centroid. As outlined before, the class centers are expected to be different from class-centroids. Hence, we focus in particular on using the Euclidean distance $\text{dist}(\mathbf{x}_i, \mathbf{x}_j) = \|\mathbf{x}_i - \mathbf{x}_j\|$, that is less sensitive to outliers. In Figure 2 we can see how the *INT* behaves for a toy dataset with 3 classes.

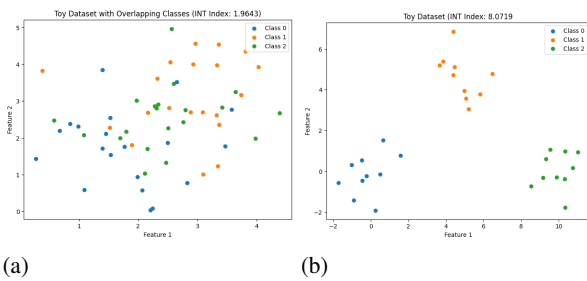


Figure 2. We show how *INT* performs with a 2D toy problem. Overlapping classes receive lower *INT* scores than well-separated clusters.

3.3. Concept Variation

Our second metric is based on concept variation (Pérez & Rendell, 1996), a measure that reflects the irregularity of

class label distributions. Understanding this variation helps to assess the structural consistency of a concept \mathcal{C} , which can be evaluated by analyzing how class labels are distributed across the feature space. A highly irregular feature space consists of numerous disjoint regions, often requiring lengthy concept representations. Conversely, a more uniform space contains expansive regions where examples share the same class labels, enabling more concise concept descriptions.

The concept variation metric v estimates the likelihood that two neighboring examples belong to distinct classes, thereby approximating the extent of irregularity in the class label distribution. However, the original definition of v is limited to Boolean spaces and assumes that all possible examples in the space are accessible.

Formally, let $\mathbf{x}_{i_1}, \dots, \mathbf{x}_{i_n}$ be the n closest neighbors at Hamming distance one of an example \mathbf{x}_i in an n -dimensional Boolean space. The concept variation for a single instance \mathbf{x}_i is defined as

$$v(\mathbf{x}_i) = \frac{1}{n} \sum_{j=1}^n \delta(y_i, y_{i_j}) \quad (3)$$

where $\delta(y_i, y_{i_j}) = 1$ if $y_i \neq y_{i_j}$, and 0 otherwise. Concept variation is computed as the average of this factor across all examples in the feature space:

$$v_{\text{total}} = \frac{1}{2^n} \sum_{i=1}^{2^n} v(\mathbf{x}_i) \in [0, 1]. \quad (4)$$

The applicability of v_{total} is limited to artificial domains where all possible examples can be generated. (Pérez & Rendell, 1996) show how the concepts with high v_{total} are difficult to learn for most conventional inductive algorithms. Since in real-world scenarios this assumption no longer holds, a distance matrix D is used to determine the contribution of each example to the amount of concept variation. The contribution to the amount of concept variation depends on the distance when $\mathbf{x}_i, \mathbf{x}_j$ differ in value by using the following function: $w_{ij} = 2^{-\alpha \cdot (D_{ij}/(\sqrt{d} - D_{ij}))}$, where α modulates the effect of distance. The higher the α , the less weight is assigned to the distance as it increases between the two examples. The upper bound is reached if $\text{dist}(\mathbf{x}_i, \mathbf{x}_j) = 0$ and the lower bound is reached when $\text{dist}(\mathbf{x}_i, \mathbf{x}_j) = \sqrt{n}$ which corresponds to the maximum distance between two examples in an n -dimensional feature space. We describe our implementation of concept variation in Algorithm 1.

Algorithm 1 Concept Variation

Input: Embedding $\phi(\mathbf{x}) \in \mathbb{R}^d$, Labels y , Hyperparameter α ,

Output: Concept variation v of each example

Step 1: Normalize Data:

Normalize $\phi(\mathbf{x})$ to $[0, 1]$, such that $\hat{\phi}(\mathbf{x}_i) \in [0, 1]$.

Step 2: Compute Pairwise Euclidean Distances:

Compute distance matrix $D \in \mathbb{R}^{n \times n}$, where $D_{ij} = \|\hat{\phi}(\mathbf{x}_i) - \hat{\phi}(\mathbf{x}_j)\|_2$.

Step 3: Compute Concept Variation:

Compute weight matrix $w \in \mathbb{R}^{n \times n}$, where $w_{ij} = 2^{-\alpha \cdot (D_{ij} / \max\{\sqrt{d} - D_{ij}, \epsilon\})}$

Set $w_{ii} = 0$ for all i to eliminate self-contributions.

Compute concept variation for each instance:

$$v(\mathbf{x}_i) = \frac{\sum_{j=1}^n w_{ij} \cdot \delta(y_i, y_j)}{\sum_{j=1}^n w_{ij}}.$$

We use the standard deviation of v for transferability estimation:

$$\sigma_v = \sqrt{\frac{1}{n} \sum_{i=1}^n (v(\mathbf{x}_i) - \bar{v})^2}; \quad \bar{v} = \frac{1}{n} \sum_{i=1}^n v(\mathbf{x}_i) \quad (5)$$

A higher standard deviation in concept variation indicates greater diversity in how individual examples’ labels differ from their neighbors across the dataset. In other words, some points may be surrounded by mostly similar labels (low concept variation) while others see very mixed labels (high concept variation), making the overall distribution of concept variation more spread out.

4. Experiments and Results

In this section, we evaluate our metrics against the current state-of-the-art SITE metrics in image classification (Section 4.1), image classification with a low data regime (Section 4.2), self-supervised learning (Section 4.3), source selection (Section 4.4) and larger network size (Section 4.5). We also provide ablation studies in Section 4.6 and Section 4.7.

Fine-Tuning Implementation details We can obtain the ground-truth ranking by fine-tuning all pre-trained models with hyper-parameters sweeping on target datasets. We use a similar fine-tuning setup as SFDA (Shao et al., 2022) for our experiments. To obtain test accuracies, we fine-tune pre-trained models with a grid search over learning rates $\{10^{-1}, 10^{-2}, 10^{-3}, 10^{-4}\}$ and a weight decay in $\{10^{-3}, 10^{-4}, 10^{-5}, 10^{-6}, 0\}$ with early stopping. We determine the best hyper-parameters based on the validation set, and fine-tune the pre-trained model on the target dataset with this parameter and without early stopping. The resulting test accuracy is used as the ground truth score G_m for model Φ_m . This way, we obtain a set of scores $\{G_m\}_{m=1}^M$ as the

ground truth to evaluate our pre-trained model rankings. To compute our metrics, we first perform a single forward pass of the pre-trained model through all target examples to extract their features. We compute the interclass distances with the Euclidean distance metric and we use the default value of $\alpha = 2$ as defined by (Pérez & Rendell, 1996) for our second metric. We provide the implementation of our metrics in Appendix D, together with the wall clock time analysis (Experiment 4.8).

Following the previous works (Shao et al., 2022; You et al., 2021; Li et al., 2021b) we use weighted Kendall’s tau τ (Vigna, 2015) to evaluate the effectiveness of transferability metrics. Kendall’s tau τ returns the ratio of concordant pairs minus discordant pairs when enumerating all $\binom{M}{2}$ pairs of $\{T_m\}_{m=1}^M$ and $\{G_m\}_{m=1}^M$ as given by:

$$\tau = \frac{2}{M(M-1)} \sum_{1 \leq i \leq j \leq M} \text{sgn}(G_i - G_j) \text{sgn}(T_i - T_j) \quad (6)$$

Where $\text{sgn}(x)$ is the signum function returning 1 if $x > 0$ and -1 otherwise. In the weighted version of Kendall’s tau τ_ω , the ranking performance of top-performing models is measured to evaluate transferability metrics. In principle, a higher τ_ω indicates that the transferability metric produces a better ranking for pretrained models.

4.1. Experiment 1: Image Classification

We propose a new and challenging experimental setup for the transferability assessment of neural networks. We use the following datasets for our experiments from the Meta-Album suite (Ullah et al., 2022): Flowers (Nilsback & Zisserman, 2008), Plant Village (G. & J., 2019), DIBaS (Zielinski et al., 2017), RESISC (Cheng et al., 2017), Cars (Krause et al., 2013), Textures (Fritz et al., 2004), and 100-sports (Piosenka). For our pre-trained model zoo we use Data-efficient Image Transformer (DeiT) (Touvron et al., 2020), Co-scale Conv-Attentional Image Transformer (CoaT) (Xu et al., 2021), Multi-Axis Vision Transformer (MaxViT) (Tu et al., 2022), MobileViT (Mehta & Rastegari, 2022), Multi-scale Vision Transformer (MViT) (Fan et al., 2021), and Cross-Covariance Image Transformer (XCiT) (El-Nouby et al., 2021) pretrained on ImageNet-1k from Huggingface timm library (Wightman, 2019). For image classification tasks, we select LogMe, SFDA, N-LEEP, ETran, LDA Baseline (LDA was available with ETran codebase), NCTI, and TransRate. We describe our model zoo and dataset selection, along with the limitations of the current experimental design, in detail in Appendix B.3.

The results in Table 1 show the effectiveness of our methods for datasets with INT achieving the highest average τ_ω . INT seems to outperform on every dataset except DIBaS.

Occam’s model: Selecting simpler representations for better transferability estimation

Dataset Metric	DIBaS	Flowers	Sports	Plants	Textures	Cars	RESISC	Average
LogMe	-0.49	-0.45	-0.45	0.09	-0.26	-0.40	-0.37	-0.33
SFDA	-0.09	-0.17	-0.17	0.21	-0.26	-0.07	-0.17	-0.11
LDA	0.59	0.09	-0.14	0.27	0.07	-0.25	0.09	0.10
N-LEEP	-0.22	-0.53	-0.60	-0.15	-0.10	-0.60	-0.53	-0.39
ETran	0.86	0.28	0.19	0.46	0.57	0.10	0.09	0.37
TransRate	0.34	0.31	0.31	0.32	0.84	0.18	0.38	0.38
NCTI	0.14	-0.37	-0.37	-0.07	-0.51	-0.26	-0.53	-0.28
Concept Variance(ours)	0.03	0.52	0.52	0.13	0.04	-0.06	0.93	0.30
<i>INT</i> (ours)	0.62	0.77	0.77	0.41	0.87	0.61	0.84	0.70
Concept Variance+INT(ours)	0.56	0.93	0.93	0.83	0.04	0.52	0.93	0.68

Table 1. Weighted Kendall’s τ_ω of LogMe SFDA LDA N-LEEP, ETran, TransRate and NCTI vs *INT* and Concept Variation (the higher the better) in limited data settings.

4.2. Experiment 2: Limited data setting

In a realistic transfer learning setting, we have only a small amount of data available for the target task. To emulate this more challenging setting, we perform an experiment with a limited set of 40 examples per class, reported in Table 2. Here as well, we observe that Concept Variance performs much more robustly than other baseline methods and also with respect to *INT* in the DIBaS and Flowers dataset. The combination of both *INT* and Concept Variation where the classes are balanced with a limited set of examples. We observe that *INT* obtains the highest score as well in this scenario and Concept Variance obtains the second highest score in this scenario. We also observe that the sum of *INT* with Concept Variance obtains higher τ_ω than *INT* or Concept Variance separately.

4.3. Experiment 3: SSL Experiments

For our third set of experiments, we apply our metrics to the Self-Supervised Learning(SSL) task. For self-supervised learning we use BYOL (Grill et al., 2020), Deepcluster-v2 (Caron et al., 2018), Infomin (Tian et al., 2020), In-Dis (Wu et al., 2018), MoCo-v1 (He et al., 2020), MoCo-v2 (He et al., 2020), PCL-v1, PCL-v2 (Li et al., 2021a), Sela-V2 (YM. et al., 2020) and SWAV (Caron et al., 2020) with a pretrained ResNet-50 backbone. We use CIFAR10, CIFAR100 (Krizhevsky et al., 2009) and Caltech101 (Fei-Fei et al., 2007) for our experiments.¹ We report the τ_ω of LogMe, SFDA and our metrics in Table 3. In SSL experiments we show that *INT* works on par with SFDA with a tiny difference of average τ_ω of 0.752 whereas SFDA average τ_ω is 0.749. We did not get result on TransRate for the other two datasets after 120 minutes of compute for the other two datasets.

¹We use setup and code from the SFDA (Shao et al., 2022) Github repository that is in turn adapted from Ericsson et al. (2021) and report the performance in Table 3.

Dataset Metric	Caltech101	CIFAR10	CIFAR100	Avg
LogMe	0.55	0.42	0.15	0.379
SFDA	0.61	0.85	0.79	0.749
TransRate	-	0.77	-	-
CV(ours)	-0.36	0.24	-0.26	-0.120
<i>INT</i> (ours)	0.67	0.83	0.76	0.752

Table 3. Experiments on SSL methods comparing *INT*, Concept Variance(CV), LogMe and SFDA

4.4. Experiment 4: Source Selection

In this experiment, we evaluate whether our proposed transferability estimate works well if our source models are trained on more specific source datasets (e.g., where all classes belong to one domain), as opposed to very broad source datasets, such as ImageNet. We use the models CoaT, DeiT, MAXVit, MViTv2, and XciT pre-trained on ImageNet-1k and then fine-tuned on the following datasets: Flowers, RESISC, DIBaS, and Plant Village. Our resulting model zoo consists of 24 models. The target datasets in this experiment are Sports, Textures, and Cars. We report the performance for this experiment in Table 4. We observe that *INT* performs here together with TransRate best.

Dataset Metric	Sports	Textures	Cars	Average
LogMe	0.384	0.477	0.325	0.395
TransRate	0.433	0.158	0.800	0.464
<i>INT</i> (ours)	0.441	0.223	0.723	0.464

Table 4. Source selection results comparing *INT*, TransRate and LogMe

4.5. Experiment 5: Bigger Networks

In this experiment, we evaluate bigger models with larger embedding sizes as well as parameter range. We take the

Dataset Metric	DIBaS	Flowers	Sports	Plants	Textures	Cars	RESISC	Average
LogMe	0.42	-0.25	-0.53	-0.07	-0.02	-0.53	-0.37	-0.19
SFDA	-0.41	0.27	0.05	-0.01	0.06	0.19	0.12	0.04
LDA	-0.25	-0.08	-0.29	-0.02	0.52	-0.15	-0.12	-0.06
N-LEEP	0.21	-0.37	-0.53	-0.47	0.13	-0.60	-0.45	-0.30
ETran	0.05	0.06	0.21	0.16	0.80	0.21	0.18	0.24
TransRate	-0.24	0.12	0.31	0.27	0.41	0.31	0.40	0.23
NCTI	0.15	-0.53	-0.53	0.02	-0.12	-0.53	-0.36	-0.27
Concept Variance(ours)	0.87	0.73	0.27	0.17	-0.10	0.28	0.73	0.42
<i>INT</i> (ours)	-0.24	0.52	0.77	0.66	0.62	0.77	0.91	0.57
Concept Variance+INT(ours)	0.62	0.62	0.73	0.79	0.39	0.70	0.73	0.65

Table 2. Weighted Kendall's τ_ω of LogMe SFDA LDA N-LEEP, ETran, TransRate, and NCTI vs *INT* and Concept Variation (the higher the better) in the limited data setting.

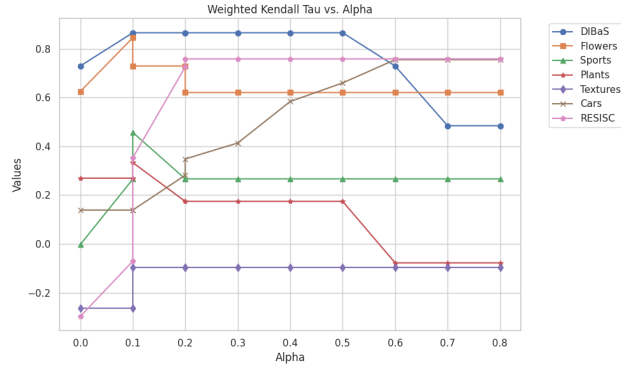


Figure 3. Alpha α studies

larger version of models introduced in Section 4.1, details of selected models can be found in Appendix B.2. The embedding size also quadruples in most of the models. We report our findings for this experiment in Table 5. We observe every metric performance drop in this scenario. This also implies that it is harder to estimate the representational complexity when embeddings are larger. Our methods still show much better performance than other metrics. The performance is notably worse for the DIBaS and Cars datasets, where every metric yields a negative τ_ω . We found that this decline is primarily due to two networks that performed exceptionally poorly, achieving accuracies between 10-35%—the lowest observed across all networks and datasets.

4.6. Experiment 6: Effect of α on Concept Variance

We analyze the effect of class weights on Concept Variance performance. We show the effect of α in Figure 3. The results suggest that the optimal α value is between 2-5.

4.7. Experiment 7: *INT* distance metric studies

In this study, we analyze how *INT* performs under various distance metrics. We compare the following metrics: Euclidean, Squared Euclidean, Manhattan, and Cosine. We used the implementations of the pairwise distances from the CuML (Raschka et al., 2020) and CuPy (Okuta et al., 2017) libraries. We report the performance of *INT* with different distance metrics in Table 6. We observe that Euclidean gives the most optimal performance out of all very close to squared Euclidean with the difference in the Textures dataset. Cosine distance reports the worst performance with negative τ_ω .

4.8. Experiment 8: Wall clock analysis/time taken

We benchmark the computation time for scoring MVItv2 Base on the DIBaS dataset. We observe that our metrics provide better performance than second and third-best performing metrics(Transrate and SFDA) in a fraction of time with *INT* performing 5 times faster than SFDA and 43 times better than TransRate and Concept Variance performing 30 times faster than SFDA and 280 times faster than TransRate, making these metrics suitable for large scale assessment of pretrained models.

Metric	Time(s)
LogMe	0.43
SFDA	6.32
TransRate	56.35
<i>INT</i> (ours)	1.28
Concept Variance(ours)	0.20

Table 7. Wall clock benchmarking of different top-performing metrics (in seconds).

Dataset Metric	DIBaS	Flowers	Sports	Plants	Textures	Cars	RESISC	Average
LogMe	-0.33	-0.90	-0.53	-0.05	0.53	-0.49	-0.23	-0.29
SFDA	-0.22	-0.05	0.25	0.84	0.44	-0.49	0.19	0.14
LDA	-0.14	-0.25	-0.06	0.73	0.63	-0.75	-0.22	-0.01
ETran	-0.53	-0.30	-0.43	0.72	0.52	-0.79	-0.27	-0.16
TransRate	-0.21	-0.35	-0.13	0.69	0.63	-0.61	-0.14	-0.02
NCTI	0.02	-0.59	-0.09	-0.25	0.08	-0.36	-0.18	-0.19
<i>INT</i>	-0.21	0.40	0.41	0.80	0.63	-0.49	0.05	0.23
Concept Variation	0.90	0.58	0.46	-0.15	0.13	-0.05	-0.53	0.19

Table 5. Experiment on Larger Networks

Dataset Distance	DIBaS	Flowers	Sports	Plants	Textures	Cars	RESISC	Average
Euclidean	0.62	0.77	0.77	0.41	0.87	0.61	0.84	0.70
Squared Euclidean	0.62	0.77	0.77	0.41	0.79	0.61	0.84	0.69
Manhattan	0.61	0.62	0.62	0.54	0.77	0.50	0.70	0.62
Cosine	0.09	-0.35	-0.35	-0.28	0.43	-0.50	-0.16	-0.16

 Table 6. Extended *INT* Ablation study

5. Conclusion and Discussion

With the current proliferation of pretrained models, finding the best model for a given target task becomes an increasingly important component of transfer learning. In this work, we propose two novel transferability metrics for classification tasks that are based on the idea that the ‘simplest’ representation, i.e. the one that leads to the clearest separation of classes, will be the best starting point for future finetuning. We evaluate both metrics, Pairwise Normalized Interclass Distance (*INT*) and Concept Variance, on a wide set of in-depth experiments across many image classification problems. We find that the *INT* metric significantly outperforms all of the state-of-the-art transferability metrics (by 38% in Experiment 4.1 and 33% in Experiment 4.2), although depending on the target task, Concept Variance or a combination of both works better. Moreover, both metrics can be computed efficiently, faster or on par with existing methods.

5.1. Future work

An important direction for future work is extending transferability metrics to tasks beyond classification, such as object detection, keypoint regression, semantic segmentation, and depth estimation. These tasks pose unique challenges, as they require processing continuous and multidimensional target variables rather than discrete labels. Nevertheless, we believe that metrics that are similarly based on the complexity of the pre-trained embeddings can provide valuable

insights and improvements for pretrained model selection and transfer learning in these domains as well.

Impact Statement

This paper presents the work around transferability estimation and its links to simplicity of representations. Our work can help in reducing the time taken by ML practitioners to select a pretrained model hence also reducing computational costs of training multiple models and reducing carbon footprint of a ML workflow.

References

Bao, Y., Li, Y., Huang, S.-L., Zhang, L., Zheng, L., Zamir, A., and Guibas, L. An information-theoretic approach to transferability in task transfer learning. In *2019 IEEE International Conference on Image Processing (ICIP)*, pp. 2309–2313, 2019. doi: 10.1109/ICIP.2019.8803726. [2](#)

Bezdek, J. and Pal, N. Some new indexes of cluster validity. *IEEE Transactions on Systems, Man, and Cybernetics, Part B (Cybernetics)*, 28(3):301–315, 1998. doi: 10.1109/3477.678624. [3](#)

Caron, M., Bojanowski, P., Joulin, A., and Douze, M. Deep clustering for unsupervised learning of visual features. In *European Conference on Computer Vision*, 2018. [6](#)

Caron, M., Misra, I., Mairal, J., Goyal, P., Bojanowski, P., and Joulin, A. Unsupervised learning of visual features by contrasting cluster assignments. In *Advances in Neural Information Processing Systems*. Curran Associates, Inc., 2020. 6

Cheng, G., Han, J., and Lu, X. Remote sensing image scene classification: Benchmark and state of the art. *CoRR*, abs/1703.00121, 2017. URL <http://arxiv.org/abs/1703.00121>. 5

Deng, J., Dong, W., Socher, R., Li, L.-J., Li, K., and Fei-Fei, L. Imagenet: A large-scale hierarchical image database. In *2009 IEEE Conference on Computer Vision and Pattern Recognition*, pp. 248–255, 2009. doi: 10.1109/CVPR.2009.5206848. 1, 2

Ding, Y., Jiang, B., Yu, A., Zheng, A., and Liang, J. Which model to transfer? a survey on transferability estimation, 2024. URL <https://arxiv.org/abs/2402.15231>. 3

El-Nouby, A., Touvron, H., Caron, M., Bojanowski, P., Douze, M., Joulin, A., Laptev, I., Neverova, N., Synnaeve, G., Verbeek, J., and Jégou, H. Xcit: Cross-covariance image transformers. In *Neural Information Processing Systems*, 2021. URL <https://api.semanticscholar.org/CorpusID:235458262>. 5

Ericsson, L., Gouk, H., and Hospedales, T. M. How Well Do Self-Supervised Models Transfer? In *CVPR*, 2021. URL <http://arxiv.org/abs/2011.13377>. 6

Fan, H., Xiong, B., Mangalam, K., Li, Y., Yan, Z., Malik, J., and Feichtenhofer, C. Multiscale vision transformers. *2021 IEEE/CVF International Conference on Computer Vision (ICCV)*, pp. 6804–6815, 2021. URL <https://api.semanticscholar.org/CorpusID:233346705>. 5

Fei-Fei, L., Fergus, R., and Perona, P. Learning generative visual models from few training examples: An incremental bayesian approach tested on 101 object categories. *Computer Vision and Image Understanding*, 2007. doi: <https://doi.org/10.1016/j.cviu.2005.09.012>. Special issue on Generative Model Based Vision. 6

Fritz, M., Hayman, E., Caputo, B., and Eklundh, J. The kth-tips database. 2004. URL <https://www.csc.kth.se/cvap/databases/kth-tips/index.html>. 5

G., G. and J., A. P. Identification of plant leaf diseases using a nine-layer deep convolutional neural network. *Computers and Electrical Engineering*, 76:323–338, 2019. ISSN 0045-7906. doi: <https://doi.org/10.1016/j.compeleceng.2019.04.011>. URL <https://www.sciencedirect.com/science/article/pii/S0045790619300023>. 2, 5

Gholami, M., Akbari, M., Wang, X., Kamranian, B., and Zhang, Y. Etran: Energy-based transferability estimation. In *Proceedings of the IEEE/CVF International Conference on Computer Vision*, pp. 18613–18622, 2023. 2

Grill, J.-B., Strub, F., Altché, F., Tallec, C., Richemond, P., Buchatskaya, E., Doersch, C., Avila Pires, B., Guo, Z., Gheshlaghi Azar, M., Piot, B., kavukcuoglu, k., Munos, R., and Valko, M. Bootstrap your own latent - a new approach to self-supervised learning. In *Advances in Neural Information Processing Systems*, volume 33, 2020. 6

He, K., Fan, H., Wu, Y., Xie, S., and Girshick, R. Momentum contrast for unsupervised visual representation learning. In *2020 IEEE/CVF Conference on Computer Vision and Pattern Recognition (CVPR)*, 2020. doi: 10.1109/CVPR42600.2020.00975. 6

Hess, S., Duivesteijn, W., and Mocanu, D. Softmax-based classification is k-means clustering: Formal proof, consequences for adversarial attacks, and improvement through centroid based tailoring. *arXiv preprint arXiv:2001.01987*, 2020. 12

Ho, T. K. and Basu, M. Complexity measures of supervised classification problems. *IEEE Transactions on Pattern Analysis and Machine Intelligence*, 24(3):289–300, 2002. doi: 10.1109/34.990132. 2

Huang, L.-K., Huang, J., Rong, Y., Yang, Q., and Wei, Y. Frustratingly easy transferability estimation. In *International Conference on Machine Learning*, pp. 9201–9225. PMLR, 2022. 1, 2

Kam Ho, T. Complexity of Representations in Deep Learning . In *2022 26th International Conference on Pattern Recognition (ICPR)*, pp. 2657–2663, Los Alamitos, CA, USA, August 2022. IEEE Computer Society. doi: 10.1109/ICPR56361.2022.9956594. URL <https://doi.ieee.org/10.1109/ICPR56361.2022.9956594>. 2

Krause, J., Stark, M., Deng, J., and Fei-Fei, L. 3d object representations for fine-grained categorization. In *4th International IEEE Workshop on 3D Representation and Recognition (3dRR-13)*, Sydney, Australia, 2013. 2, 5

Krizhevsky, A., Hinton, G., et al. Learning multiple layers of features from tiny images. 2009. 6

Li, J., Zhou, P., Xiong, C., and Hoi, S. Prototypical contrastive learning of unsupervised representations. In *International Conference on Learning Representations*, 2021a. 6

Li, X., Hu, Z., Ge, Y., Shan, Y., and Duan, L.-Y. Exploring model transferability through the lens of potential energy. In *2023 IEEE/CVF International Conference on Computer Vision (ICCV)*, 2023. doi: 10.1109/ICCV51070.2023.00500. 2

Li, Y., Jia, X., Sang, R., Zhu, Y., Green, B., Wang, L., and Gong, B. Ranking neural checkpoints. In *2021 IEEE/CVF Conference on Computer Vision and Pattern Recognition (CVPR)*, 2021b. doi: 10.1109/CVPR46437.2021.00269. 2, 5

Mehta, S. and Rastegari, M. Mobilevit: Light-weight, general-purpose, and mobile-friendly vision transformer. In *International Conference on Learning Representations*, 2022. URL <https://openreview.net/forum?id=vh-0sUt8H1G>. 5

Nguyen, C. V., Hassner, T., Seeger, M., and Archambeau, C. Leep: a new measure to evaluate transferability of learned representations. In *Proceedings of the 37th International Conference on Machine Learning, ICML'20*. JMLR.org, 2020. 2

Nilsback, M.-E. and Zisserman, A. Automated flower classification over a large number of classes. In *Indian Conference on Computer Vision, Graphics and Image Processing*, Dec 2008. 5

Okuta, R., Unno, Y., Nishino, D., Hido, S., and Loomis, C. Cupy: A numpy-compatible library for nvidia gpu calculations. In *Proceedings of Workshop on Machine Learning Systems (LearningSys) in The Thirty-first Annual Conference on Neural Information Processing Systems (NIPS)*, 2017. URL http://learningsys.org/nips17/assets/papers/paper_16.pdf. 7

Papyan, V., Han, X., and Donoho, D. L. Prevalence of neural collapse during the terminal phase of deep learning training. *Proceedings of the National Academy of Sciences*, 117(40):24652–24663, 2020. 3

Pérez, E. and Rendell, L. A. Learning despite concept variation by finding structure in attribute-based data. In *Proceedings of the Thirteenth International Conference on International Conference on Machine Learning, ICML'96*, pp. 391–399, San Francisco, CA, USA, 1996. Morgan Kaufmann Publishers Inc. ISBN 1558604197. 3, 4, 5

Piosenka, G. 100 sports image classification. URL <https://www.kaggle.com/datasets/gpiosenka/sports-classification>. 5

Raschka, S., Patterson, J., and Nolet, C. Machine learning in python: Main developments and technology trends in data science, machine learning, and artificial intelligence. *arXiv preprint arXiv:2002.04803*, 2020. 7

Rendell, L. and Cho, H. Empirical learning as a function of concept character. *Mach. Learn.*, 5(3):267–298, September 1990. ISSN 0885-6125. doi: 10.1023/A:1022651406695. URL <https://doi-org.dianus.libr.tue.nl/10.1023/A:1022651406695>. 3

Schuhmann, C., Beaumont, R., Vencu, R., Gordon, C. W., Wightman, R., Cherti, M., Coombes, T., Katta, A., Mullis, C., Wortsman, M., Schramowski, P., Kundurthy, S. R., Crowson, K., Schmidt, L., Kaczmarczyk, R., and Jitsev, J. LAION-5b: An open large-scale dataset for training next generation image-text models. In *Thirty-sixth Conference on Neural Information Processing Systems Datasets and Benchmarks Track*, 2022. URL <https://openreview.net/forum?id=M3Y74vmsMcY>. 1, 2

Shao, W., Zhao, X., Ge, Y., Zhang, Z., Yang, L., Wang, X., Shan, Y., and Luo, P. Not all models are equal: Predicting model transferability in a self-challenging fisher space. In *Computer Vision – ECCV 2022: 17th European Conference, Tel Aviv, Israel, October 23–27, 2022, Proceedings, Part XXXIV*, pp. 286–302, Berlin, Heidelberg, 2022. Springer-Verlag. ISBN 978-3-031-19829-8. doi: 10.1007/978-3-031-19830-4-17. URL https://doi-org.dianus.libr.tue.nl/10.1007/978-3-031-19830-4_17. 2, 5, 6

Tan, Y., Li, Y., and Huang, S.-L. Otce: A transferability metric for cross-domain cross-task representations. *2021 IEEE/CVF Conference on Computer Vision and Pattern Recognition (CVPR)*, 2021. 2

Tian, Y., Sun, C., Poole, B., Krishnan, D., Schmid, C., and Isola, P. What makes for good views for contrastive learning? In *Advances in Neural Information Processing Systems*. Curran Associates, Inc., 2020. 6

Touvron, H., Cord, M., Douze, M., Massa, F., Sablayrolles, A., and J'egou, H. Training data-efficient image transformers & distillation through attention. In *International Conference on Machine Learning*, 2020. 5

Tran, A., Nguyen, C., and Hassner, T. Transferability and hardness of supervised classification tasks. In *2019 IEEE/CVF International Conference on Computer Vision (ICCV)*, pp. 1395–1405, 2019. doi: 10.1109/ICCV.2019.00148. 2

Tu, Z., Talebi, H., Zhang, H., Yang, F., Milanfar, P., Bovik, A. C., and Li, Y. Maxvit: Multi-axis vision transformer. In *European Conference on Computer Vision*,

2022. URL <https://api.semanticscholar.org/CorpusID:247939839>. 5

Ullah, I., Carrion, D., Escalera, S., Guyon, I. M., Huisman, M., Mohr, F., van Rijn, J. N., Sun, H., Vanschoren, J., and Vu, P. A. Meta-album: Multi-domain meta-dataset for few-shot image classification. In *Thirty-sixth Conference on Neural Information Processing Systems Datasets and Benchmarks Track*, 2022. URL <https://meta-album.github.io/>. 5

Vigna, S. A weighted correlation index for rankings with ties. In *Proceedings of the 24th International Conference on World Wide Web*, WWW '15, Republic and Canton of Geneva, CHE, 2015. International World Wide Web Conferences Steering Committee. doi: 10.1145/2736277.2741088. 5

Wang, Z., Luo, Y., Zheng, L., Huang, Z., and Baktashmotlagh, M. How far pre-trained models are from neural collapse on the target dataset informs their transferability. In *2023 IEEE/CVF International Conference on Computer Vision (ICCV)*, 2023. doi: 10.1109/ICCV51070.2023.00511. 2

Wightman, R. Pytorch image models. <https://github.com/rwightman/pytorch-image-models>, 2019. 5

Wu, Z., Xiong, Y., Yu, S. X., and Lin, D. Unsupervised feature learning via non-parametric instance discrimination. In *2018 IEEE/CVF Conference on Computer Vision and Pattern Recognition*, 2018. doi: 10.1109/CVPR.2018.00393. 6

Xu, W., Xu, Y., Chang, T. A., and Tu, Z. Co-scale conv-attentional image transformers. 2021 *IEEE/CVF International Conference on Computer Vision (ICCV)*, pp. 9961–9970, 2021. URL <https://api.semanticscholar.org/CorpusID:233219797>. 5

YM., A., C., R., and A., V. Self-labelling via simultaneous clustering and representation learning. In *International Conference on Learning Representations*, 2020. 6

You, K., Liu, Y., Long, M., and Wang, J. Logme: Practical assessment of pre-trained models for transfer learning. In *International Conference on Machine Learning*, 2021. URL <https://api.semanticscholar.org/CorpusID:231985863>. 2, 5

Zielinski, B., Plichta, A., Misztal, K., Spurek, P., Brzyczczy-Wloch, M., and Ochonska, D. Deep learning approach to bacterial colony classification. *PLOS ONE*, 12(9):1–14, 09 2017. doi: 10.1371/journal.pone.0184554. URL <https://doi.org/10.1371/journal.pone.0184554>. 5

A. Proofs

We state first the following theorem from (Hess et al., 2020) for completeness, since we need it for our analysis.

Theorem A.1. *Let $h_{W,b}(\mathbf{x}) = \text{softmax}(W\mathbf{x} + b)$ be a multinomial regression model with $W \in \mathbb{R}^{C \times d}$ and $b \in \mathbb{R}^C$, computing class predictions as $y = \arg \max_{1 \leq c \leq C} \mathbf{x}^\top W_{\cdot c} + b_c$. If W has at least a rank of $r \geq C$, then there exist C class centers $\mu_c \in \mathbb{R}^d$ such that every point \mathbf{x} is assigned to the class having the nearest center:*

$$y = \arg \min_{1 \leq c \leq C} \|\mathbf{x} - \mu_c\|^2.$$

Proof. We show that for any dataset and network there exists a set of class centers such that the classification does not change when classifying according to the nearest center.

We gather given data points in the matrix D :

$$D^\top = (\mathbf{x}_1 \quad \dots \quad \mathbf{x}_N) \in \mathbb{R}^{d \times N}.$$

We define $Z = W + \mathbf{v}\mathbf{1}_C^\top$, where $\mathbf{v} \in \mathbb{R}^d$ and $\mathbf{1}_C \in \{1\}^C$ is a constant one vector. The (soft)max classification of all data points in D is then given by the one-hot encoded matrix $Y \in \{0, 1\}^{N \times C}$ that optimizes the objective

$$\arg \max_Y \text{tr}(Y(W^\top D^\top + \mathbf{b}\mathbf{1}_N^\top)) = \arg \min_Y \|D - YZ^\top\|^2 + \text{tr}((2\mathbf{b}\mathbf{1}_C^\top - Z^\top Z)Y^\top Y) \quad (7)$$

The matrix $Z \in \mathbb{R}^{d \times C}$ indicates a set of C centers by its columns. The first term of Equation (7) is minimized if Y assigns the class with the closest centroid to each data point in D . Hence, if we can show that there exists a vector $v \in \mathbb{R}^d$ such that the second term of Equation (7) is equal to zero (given D and W) then we have shown what we wanted to prove. Since $|Y_{\cdot j}| = 1$ (every point is assigned to exactly one class), the matrix $Y^\top Y$ is a diagonal matrix, having the number of data points assigned to each class on the diagonal: $Y^\top Y = \text{diag}(|Y_{\cdot 1}|, \dots, |Y_{\cdot C}|)$. Hence, the trace term on the right of Equation (7) equals

$$\sum_{c=1}^C (2\mathbf{b}\mathbf{1}_C^\top - Z^\top Z)_{cc} |Y_{\cdot c}| = \sum_{c=1}^C (2b_c - \|W_{\cdot c}\|^2 - 2v^\top W_{\cdot c}) |Y_{\cdot c}| - \|\mathbf{v}\|^2 m \quad (8)$$

We define the vector $\mathbf{u} \in \mathbb{R}^C$ such that $u_c = b_c - \frac{1}{2}\|W_{\cdot c}\|^2$. The right term of Equation (8) is constant for a vector \mathbf{v} satisfying $u_c = \mathbf{v}^\top W_{\cdot c}$ for $1 \leq c \leq C$. That is, we need to solve the following equation for \mathbf{v} :

$$\mathbf{u} = W^\top \mathbf{v} = V \Sigma U^\top \mathbf{v}.$$

Since the rank of W is C (full column rank), this equation has a solution. It is given by the SVD of $W = U\Sigma V^\top$, where $U \in \mathbb{R}^{d \times C}$ is a left orthogonal matrix ($U^\top U = I$), $\Sigma \in \mathbb{R}_+^{C \times C}$ is a diagonal matrix having only positive values, and $V \in \mathbb{R}^{C \times C}$ is an orthogonal matrix ($V^\top V = VV^\top = I$). Setting $\mathbf{v} = U\Sigma^{-1}V^\top \mathbf{u}$, this vector solves the equation. \square

Theorem A.2 (Restatement of Thm 3.1). *For any multinomial regression model $h_{W,b}(\mathbf{z}) = \text{softmax}(W\mathbf{z} + b)$ exist class centers μ_1, \dots, μ_C such that*

$$h_{W,b}(\mathbf{x})_y = \frac{\exp(-\frac{1}{2}\|\mathbf{x} - \mu_y\|^2)}{\sum_{c=1}^C \exp(-\frac{1}{2}\|\mathbf{x} - \mu_c\|^2)}$$

Proof. According to the proof of Thm. A.1, exists a vector \mathbf{v} such that the class boundaries do not change when we replace the standard multinomial regression prediction with the nearest center prediction, where the centers are defined by $\mu_c = W_{\cdot c} + \mathbf{v}$. For this set of centroids we have the following relationship of the multinomial regression confidence to the

center-based confidence.

$$\begin{aligned}
 \text{softmax}(W\mathbf{x} + \mathbf{b})_y &= \frac{\exp(\mathbf{x}^\top W_{\cdot y} + b_y)}{\sum_{c=1}^C \exp(\mathbf{x}^\top W_{\cdot c} + b_c)} \cdot \frac{\exp(\mathbf{x}^\top \mathbf{v})}{\exp(\mathbf{x}^\top \mathbf{v})} \\
 &= \frac{\exp(\mathbf{x}^\top \mu_y + b_y)}{\sum_{c=1}^C \exp(\mathbf{x}^\top \mu_c + b_c)} \\
 &= \frac{\exp(-\frac{1}{2}\|\mu_y\|^2 + \mathbf{x}^\top \mu_y + b_y + \frac{1}{2}\|\mu_y\|^2)}{\sum_{c=1}^C \exp(-\frac{1}{2}\|\mu_c\|^2 + \mathbf{x}^\top \mu_c + b_c + \frac{1}{2}\|\mu_c\|^2)} \frac{\exp(\frac{1}{2}\|\mathbf{x}\|^2)}{\exp(\frac{1}{2}\|\mathbf{x}\|^2)} \\
 &= \frac{\exp(-\frac{1}{2}\|\mu_y - \mathbf{x}\|^2) \exp(b_y + \frac{1}{2}\|\mu_y\|^2)}{\sum_{c=1}^C \exp(-\frac{1}{2}\|\mu_c - \mathbf{x}\|^2) \exp(b_c + \frac{1}{2}\|\mu_c\|^2)}
 \end{aligned}$$

Since the class boundaries of the nearest-center prediction do not change the original class boundaries, we have for any point \mathbf{x} on the decision boundary between class a and b $\text{softmax}(W\mathbf{x} + \mathbf{b})_a = \text{softmax}(W\mathbf{x}_2 + \mathbf{b})$. At the same time we have $\exp(-\frac{1}{2}\|\mu_{y_1} - \mathbf{x}\|^2) = \exp(-\frac{1}{2}\|\mu_{y_2} - \mathbf{x}\|^2)$ because the nearest center classifier with centers μ_c is not changing the decision boundary according to Thm A.1. As a result we have (using the equivalence above)

$$\exp(b_{y_1} + \frac{1}{2}\|\mu_{y_1}\|^2) = \exp(b_{y_2} + \frac{1}{2}\|\mu_{y_2}\|^2).$$

Since this equation holds for any point on the decision boundary, we have proven our final result. \square

B. Omitted Experiment Details in Section 4

B.1. Dataset details

- DIBaS:** Digital Image of Bacterial Species (DIBaS). The Digital Images of Bacteria Species dataset (DIBaS) (<https://github.com/gallardorafael/DIBaS-Dataset>) is a dataset of 33 bacterial species with around 20 images for each species.
- Flowers:** Flowers dataset from Visual Geometry Group, University of Oxford. The Flowers dataset(<https://www.robots.ox.ac.uk/~vgg/data/flowers/102/index.html>) consists of a variety of flowers gathered from different websites and some are photographed by the original creators. These flowers are commonly found in the UK. The images generally have large scale, pose and light variations. Some categories of flowers in the dataset has large variations of flowers while other have similar flowers in a category.
- Sports:** The 100-Sports dataset(<https://www.kaggle.com/datasets/gpiosenka/sports-classification>) is a collection of sports images covering 73 different sports. Images are 224x224x3 in size and in .jpg format. Images were gathered from internet searches. The images were scanned with a duplicate image detector program and all duplicate images were removed.
- Plants:** The Plant Village dataset <https://data.mendeley.com/datasets/tywbtsjrv/1> contains camera photos of 17 crop leaves. The original image resolution is 256x256 px. This collection covers 26 plant diseases and 12 healthy plants.
- Textures:** The original Textures dataset is a combination of 4 texture datasets: KTH-TIPS and KTH-TIPS 2 (<https://www.csc.kth.se/cvap/databases/kth-tips/index.html>), Kylberg Textures Dataset (<http://www.cb.uu.se/~gustaf/texture/>) and UIUC Textures Dataset. The data in all four datasets is collected in laboratory conditions, i.e., images were captured in a controlled environment with configurable brightness, luminosity, scale and angle. The KTH-TIPS dataset was collected by Mario Fritz and KTH-TIPS 2 dataset was collected by P. Mallikarjuna and Alireza Tavakoli Targhi, created in 2004 and 2006 respectively. Both of these datasets were prepared under the supervision of Eric Hayman and Barbara Caputo. The data for Kylberg Textures Dataset and UIUC Textures Dataset data was collected by the original authors of these datasets in September 2010 and August 2005 respectively.
- Cars:** The original Cars dataset (https://ai.stanford.edu/~jkrause/cars/car_dataset.html) was collected in 2013, and it contains more than 16 000 images from 196 classes of cars. Most images are on the road, but some have different backgrounds, and each image has only one car. Each class can have 48 to 136 images of variable resolutions.

7. **RESISC**: RESISC45 dataset(<https://gcheng-nwpu.github.io/>) gathers 700 RGB images of size 256x256 px for each of 45 scene categories. The data authors strive to provide a challenging dataset by increasing both within-class diversity and between-class similarity, as well as integrating many image variations. Even though RESISC45 does not propose a label hierarchy, it can be created from other common aerial image label organization scheme.
8. **CIFAR10**: The dataset contains 60,000 color images in 10 classes, with each image in the size of 32x32. Each class has 5,000 training samples and 1,000 testing samples.
9. **CIFAR 100**: The dataset is the same as CIFAR-10 except that it has 100 classes each of which contains 500 training images and 100 testing images. DTD (Cimpoi et al., 2014) The dataset consists of
10. **CALTECH 101**: The dataset contains 9,146 images from 101 object categories. The number of images in each category is between 40 and 800.

B.2. Models

Pretrained **timm** models used in Experiment 4.1, Experiment 4.2, Experiment 4.6 and Experiment 4.7.

Model Name	Parameters (M)	FLOPs (GMACs)	Input Resolution
CoaT Lite Tiny	5.7	1.6	224 x 224
DeiT Tiny Patch16 224	5.7	1.3	224 x 224
MaxViT Tiny TF 224	30.9	5.6	224 x 224
MobileViT XS	2.3	0.7	256 x 256
MViTv2 Tiny	5.1	1.1	224 x 224
XCiT Tiny 12 P8 224	6.7	4.8	224 x 224
MobileViTv2 100	3.6	0.9	256 x 256

Table 8. Details of the selected models from Hugging Face.

Pretrained timm models used in Section 4.5

Model Name	Parameters (M)	FLOPs (GMACs)	Input Resolution
DeiT Base Patch16 224	86.6	17.6	224 x 224
MobileViTv2 200	6.9	1.7	256 x 256
XCiT Small 12 P8 224	26.3	9.1	224 x 224
MaxViT Small TF 224	69.0	11.7	224 x 224
MViTv2 Base	51.5	10.2	224 x 224
CoaT Lite Medium 384	20.0	4.0	384 x 384

Table 9. Details of the bigger models from Hugging Face.

B.3. Experimental design

We use different search space as compared to the one in recent works such as SFDA, TransRate and ETran, We use a more realistic experimental search space, we limit out model sizes from 5-25M parameters for Experiment 4.1, 4.2, 4.5. We select models from top performing networks from PaperWithCode leaderboard on ImageNet Classification <https://paperswithcode.com/sota/image-classification-on-imagenet>. We also select every target domain dataset form a different domain. Our model search space is more complex, older works have used only 3 variants of models in different sizes which can show more models but in the end larger models eg Resnet 150 always outperform Resnet18 under similar training regimes as one can verify from the test scores(We verify this by looking at the same performance metrics used by SFDA, Etran and PED <https://github.com/mgholamikn/ETran/blob/main/tw.py>). So one can just use embedding size as a transferability metric and get a positive/better performing τ_w). Our datasets are also larger and have larger image sizes as well(128x128). Our reasoning behind the suggested experiment design is that one usually is not trying to select between a 50M parameter model and a 250M parameter model, overparameterized model

from the same family tend to work better but different models under same parameter limit is the right case where one need transferability estimation. We make sure we have no network which consistently perform worse than other networks and avoid models from same families. The model training and fine tuning is performed on single V100 GPU and metric calculation is done on single NVIDIA RTX A6000 GPU.

C. Time complexity analysis

C.1. INT

$\mathcal{O}(k^2 \cdot N^2, D)$ Where k is the number of classes, N is the number of samples and D is the embedding size of the network. Assuming $k \ll N$ the overall complexity of INT is $\mathcal{O}(N^2 \cdot D)$.

C.2. Concept Variation

The overall complexity for concept variation v is $\mathcal{O}(N^2 \cdot D)$.

D. Python Code for INT and concept variance

```

import cupy as cp
import numpy as np
from itertools import combinations
from cuml.metrics import pairwise_distances

def ft_int_gpu(N, y, dist_metric="euclidean"):

    N_gpu = cp.array(N)
    y_gpu = cp.array(y)

    # Get unique classes
    classes = np.unique(y) # Use NumPy for unique classes since it's small
    class_num = len(classes)

    if class_num == 1:
        return np.nan

    # Compute pairwise normalized interclass distances
    pairwise_norm_intercls_dist = []
    for id_cls_a, id_cls_b in combinations(range(class_num), 2):
        group_a = N_gpu[y_gpu == classes[id_cls_a]]
        group_b = N_gpu[y_gpu == classes[id_cls_b]]
        dists = pairwise_distances(group_a, group_b, metric=dist_metric)
        pairwise_norm_intercls_dist.append(cp.sum(dists) / dists.size)

    # INT computation
    norm_factor = 2.0 / (class_num * (class_num - 1.0))
    sum_intercls_dist = cp.sum(cp.array(pairwise_norm_intercls_dist))

    return float(sum_intercls_dist * norm_factor)

def precompute_concept_dist_gpu(N, concept_dist_metric):
    # Convert numpy array to CuPy array
    N = cp.asarray(N)

    # Normalize N to range [0, 1]

```

```

scaler = cuml.preprocessing.MinMaxScaler(feature_range=(0, 1))
N = scaler.fit_transform(N)

# Compute pairwise Euclidean distances using cuML
concept_distances = cuml.metrics.pairwise_distances(N, metric="euclidean")

return concept_distances

def ft_conceptvar_gpu(
    N: np.ndarray,
    y: np.ndarray,
    conceptvar_alpha: float = 2.0,
    concept_dist_metric: str = "euclidean",
    concept_minimum: float = 1e-10,
) -> t.Tuple[float, cp.ndarray]:
    # Convert numpy arrays to CuPy arrays

    N = cp.asarray(N)
    y = cp.asarray(y)

    concept_distances = precompute_concept_dist_gpu(N, concept_dist_metric)

    n_col = N.shape[1]

    div = cp.sqrt(cp.array(n_col)) - concept_distances
    div = cp.clip(div, a_min=concept_minimum, a_max=None)
    weights = cp.power(2, -conceptvar_alpha * (concept_distances / div))
    cp.fill_diagonal(weights, 0.0)

    rep_class_matrix = cp.expand_dims(y, 0).repeat(y.shape[0], axis=0)
    class_diff = (rep_class_matrix.T != rep_class_matrix).astype(cp.float32)
    w2 = weights * class_diff
    conceptvar_by_example = cp.sum(w2, axis=0) / cp.sum(weights, axis=0)
    std_dev = cp.std(conceptvar_by_example).item()

return std_dev

```

E. Additional Tables

Dataset	DIBaS	Flowers	Sports	Plants	Textures	Cars	RESISC	Average
Alpha								
$\alpha = 0.5$	0.73	0.62	-0.00	0.27	-0.26	0.14	-0.30	0.17
$\alpha = 1.0$	0.87	0.84	0.27	0.27	-0.26	0.14	-0.07	0.29
$\alpha = 1.5$	0.87	0.73	0.46	0.33	-0.10	0.14	0.35	0.40
$\alpha = 2.0$	0.87	0.73	0.27	0.17	-0.10	0.28	0.73	0.42
$\alpha = 2.5$	0.87	0.62	0.27	0.17	-0.10	0.35	0.76	0.42
$\alpha = 3.0$	0.87	0.62	0.27	0.17	-0.10	0.41	0.76	0.43
$\alpha = 4.0$	0.87	0.62	0.27	0.17	-0.10	0.58	0.76	0.45
$\alpha = 5.0$	0.87	0.62	0.27	0.17	-0.10	0.66	0.76	0.46
$\alpha = 6.0$	0.73	0.62	0.27	-0.08	-0.10	0.76	0.76	0.42
$\alpha = 7.0$	0.48	0.62	0.27	-0.08	-0.10	0.76	0.76	0.39
$\alpha = 8.0$	0.48	0.62	0.27	-0.08	-0.10	0.76	0.76	0.39

Table 10. Studying the affect of class weights on τ_ω on limited data setting